First-passage—time distributions and switching statistics in a bistable two-mode laser

Daan Lenstra*
Department of Physics and Astronomy, University of Rochester, Rochester, New York 14627

Surendra Singh
Department of Physics, University of Arkansas, Fayetteville, Arkansas 72701
(Received 11 February 1983)

As a result of quantum fluctuations, a bistable system will undergo spontaneous transitions from one state to the other. For a bistable two-mode laser we present a theoretical analysis of the switching statistics by treating it as a one-dimensional first-passage—time (FPT) problem for the intensity of one of the modes. The methodology is also applicable to other bistable systems, such as in optical bistability. Several new asymptotic results for the small- and large-time behavior of various FPT distributions are given. The switching-time distribution is introduced as a weighted integral over FPT distributions and asymptotic expressions for this distribution are given. Several results of Monte Carlo computer simulations of the FPT problem are presented.

I. INTRODUCTION

Recently, first-passage—time (FPT) distributions under the influence of quantum fluctuations in a bistable laser have been dealt with both theoretically and experimentally.[1–3] In these studies the statistics of switching between the two metastable states was treated as a one-dimensional FPT problem which led for the corresponding distribution function to the simple result $P(T)=\langle T\rangle^{-1}\times\exp(-T/\langle T\rangle)$, at least for values of T that are not too small (T is the first-passage—time and $\langle T\rangle$ its mean). This exponential dependence of T was found in reasonable agreement with experiment and so was the predicted dependence of $\langle T\rangle$ on the pump parameter.[1] The FPT problem has also attracted interest in different but related contexts, such as the decay of unstable equilibrium states[4] and the mean first-passage time in optical bistability.[5]

Surprisingly, the behavior of $P(T)$ for small times has received little or no attention yet. In fact, since $P(T)$ should in many cases vanish for $T=0$, substantial deviations of the above-mentioned simple exponential behavior are to be expected for small T, but no experimental study yet seems to have dealt with the switching statistics in the short-time regime. However, this is an interesting regime since the specific dynamics of the diffusion process rather than the drift are expected to be crucial here. A test on whether the switching problem can indeed be treated as a one-dimensional first-passage problem would, therefore, be more conclusive in the small-time regime than it will be for large times.

Although we will deal in this paper with the theoretical analysis of FPT distributions in a bistable two-mode laser, the methodology employed, as well as the results obtained, are also relevant to other bistable systems. Moreover, it has convincingly been demonstrated that a bistable two-mode laser is well accessible for experimental studies. Following Refs. 1 and 2, our analysis will also be based on the assumption that the statistics of the system can be described by a Fokker-Planck equation for the intensity distribution of one of the modes. For simplicity we will consider the case in which both modes have equal pump parameters so that we will be dealing with a symmetric two-mode system.

In Sec. II the problem will be formulated, various quantities of interest will be defined, and some useful relations will be derived. Throughout Sec. III our effort will be to find analytic expressions for the FPT distributions. Since the basic equation governing the distribution of first-passage times seems to be too complicated to allow exact analytic solutions, the emphasis will be on the derivation of asymptotic results, that is, for small and large times, respectively. Numerical results for a number of Monte Carlo computer calculations based on an equivalent Langevin equation for the intensity of one mode are presented in Sec. IV and compared with the asymptotic analytical expressions. In an attempt to increase the readability of Sec. III, a self-consistent part of the theory has been organized in the Appendix.

II. FORMULATION OF THE PROBLEM AND DEFINITIONS

For a two-mode laser operating under bistable conditions, the probability distribution function $\mathscr{P}(I,t)$ for the intensity I (in convenient units) of one of the modes can be shown to satisfy a Fokker-Planck type of equation[6]

$$\frac{\partial}{\partial t}\mathscr{P}(I,t)=\frac{1}{2}\frac{\partial^2}{\partial I^2}[\mathscr{D}(I)\mathscr{P}(I,t)]-\frac{\partial}{\partial I}[\mathscr{B}(I)\mathscr{P}(I,t)]\ , \tag{1}$$

where $\mathscr{D}(I)=8I$ is the diffusion coefficient and $\mathscr{B}(I)$ is the drift coefficient. An explicit expression for $\mathscr{B}$ will be given further on. The corresponding Langevin equation for the intensity $I(t)$ of the mode under consideration is given by

$$\frac{d}{dt}I(t)=\mathscr{B}(I(t))+X(t)\ , \tag{2}$$

where $X(t)$ is the randomly fluctuating Langevin force, describing the influence of quantum fluctuations. The statistical properties of $X(t)$ are such that the quantities

$$Y(\tau)=\int_t^{t+\tau} dt' X(t') \tag{3}$$

are independent of t and distributed according to a distribution function $\varphi(Y;\tau,I)$ that is characterized by

$$\langle Y\rangle = 0 , \tag{4}$$

$$\langle Y^2\rangle = 8I\tau , \tag{5}$$

$$\langle Y^r\rangle = O(\tau^2) \quad (r=3,4,\ldots) . \tag{6}$$

Furthermore, since I cannot assume negative values, φ should also satisfy

$$\varphi(Y;\tau,I)=0 \quad \text{when} \quad Y \le -I . \tag{7}$$

All of the requirements (4)–(7) can be met by taking for φ the shifted gamma distribution

$$\varphi(Y;\tau,I)=\frac{(Y+I)^{\alpha-1}e^{-(Y+I)/\beta}}{\Gamma(\alpha)\beta^{\alpha}} \quad (Y \ge -I) \tag{8}$$

where $\alpha = I/8\tau$ and $\beta = 8\tau$.

As a matter of course, both (1) and (2) with (8) are equivalent descriptions of the statistical properties of the mode intensity. Equation (2) together with the probability distribution (8) has been used in the Monte Carlo calculations to be described in Sec. IV.

The stationary solution to (1) can be written as

$$\mathscr{P}(I)=\frac{1}{Q}e^{-V(I)} , \tag{9}$$

where Q is a constant such that $\mathscr{P}$ is normalized to unity and V is the "potential" that can be associated with the mode. By equating the right-hand side of (1) to 0 and substituting (9) for $\mathscr{P}(I)$, we immediately find

$$\mathscr{B}(I)=\frac{1}{2}\frac{d}{dI}\mathscr{D}(I)+\tfrac{1}{2}\mathscr{D}(I)\frac{d}{dI}V(I) . \tag{10}$$

A general expression for $V(I)$ is given by Eq. (15b) of Ref. 2. Assuming from now on that both modes have equal pump parameters, the expression for the potential reads

$$V(I)=-\tfrac{1}{4}(\xi^2-1)I^2+\tfrac{1}{2}a(\xi-1)I - \ln\{1-\mathrm{erf}[\tfrac{1}{2}(\xi I-a)]\} , \tag{11}$$

where a is the pump parameter of the mode and ξ is the mode-coupling constant. We will assume that ξ has a value between 1 and 2. In Fig. 1 the potential is drawn as a function of I/a for several values of a ranging from $a=4$ to 12, assuming the coupling constant $\xi=2$.

Using (10) and (11) we easily find

$$\mathscr{B}(I)=4+2(\xi^2-1)I^2-2a(\xi-1)I - \frac{4\xi I}{\sqrt{\pi}}\frac{\exp[-\tfrac{1}{4}(\xi I-a)^2]}{1-\mathrm{erf}[\tfrac{1}{2}(\xi I-a)]} . \tag{12}$$

Various plots of the drift coefficient as a function of I/a are given in Fig. 2 for different values of a, assuming $\xi=2$. Generally, the zeros of $\mathscr{B}(I)$ correspond to stationary solutions of the corresponding deterministic equation of motion, i.e., $\dot{I}=\mathscr{B}(I)$. For $a \gtrsim 6$, and provided that ξ is not too close to 1, there are always three zeros, two of which correspond to stable equilibrium states while the other corresponds to an unstable equilibrium. It can be seen from Fig. 2 that the stable equilibrium states are characterized by intensities close to 0 (the "off" state) and close to a (the "on" state), respectively, while the unstable equilibrium has an intensity close to $a/3$. Denoting the latter intensity by I_B, we have

$$I_B \simeq \frac{a}{\xi+1}-\frac{2}{(\xi-1)a}+O\left[\frac{1}{a^2}\right] . \tag{13}$$

The intensity I_B can be thought of as separating the on and off states in the following sense: The mode under consideration will be said to be in the off state whenever its intensity is found to have a value smaller than I_B, whereas it will be said to be in the on state otherwise.

An important quantity associated with the switching behavior of the mode is the first-passage time $T(I_1,I_2)$, i.e., the time it takes for the intensity, initially equal to I_1, to assume the value I_2 for the first time under the combined influence of drift and diffusion. The distribution of these times defines a probability distribution function $P(T;I_1,I_2)$ which, by definition, is given by $(I_2 > I_1)$

$$P(T;I_1,I_2)=-\frac{\partial}{\partial T}\int_0^{I_2} dI\, \mathscr{P}(I,T) , \tag{14}$$

where $\mathscr{P}(I,T)$ is the solution of (1) subject to the conditions

$$\mathscr{P}(I,0)=\delta(I-I_1) \tag{15}$$

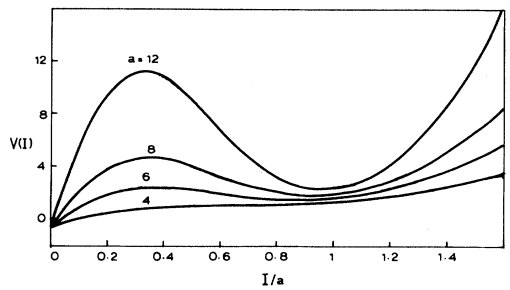

FIG. 1. Potential $V(I)$ vs I/a for several values of the pump parameter a as indicated and coupling constants $\xi=2$.

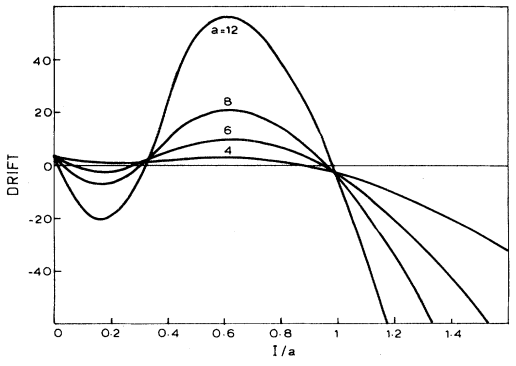

FIG. 2. Drift $\mathscr{B}(I)$ vs I/a for several values of a as indicated and coupling constant $\xi=2$.

and

$$\mathscr{P}(I_2,T)=0\ . \tag{16}$$

With the use of (1), (14), (15), and (16) it can easily be shown that $P(T;I_1,I_2)$ satisfies the adjoint Fokker-Planck equation (see also Ref. 7)

$$\frac{\partial}{\partial T}P(T;I_1,I_2) = \left[\tfrac{1}{2}\mathscr{D}(I_1)\frac{\partial^2}{\partial I_1^2}+\mathscr{B}(I_1)\frac{\partial}{\partial I_1}\right]P(T;I_1,I_2)\ , \tag{17}$$

subject to the conditions

$$P(T;I_2,I_2)=\delta(T) \tag{18}$$

and

$$\frac{\partial}{\partial T}P(T;0,I_2)=\mathscr{B}(0)\frac{\partial}{\partial I_1}P(T;I_1,I_2)\bigg|_{I_1=0}\ . \tag{19}$$

Related to P is another first-passage–time distribution function $\rho(T;I_1,I_2)$ that we will define as

$$\rho(T;I_1,I_2)=\frac{\int_0^{I_1}dI\,\mathscr{P}(I)P(T;I,I_2)}{\int_0^{I_1}dI\,\mathscr{P}(I)}\ , \tag{20}$$

where $\mathscr{P}(I)$ is the stationary intensity distribution (9). It is assumed in (20) that $0<I_1<I_2$. ρ is the distribution function of first-passage times at I_2 if the initial intensity is distributed between 0 and I_1 according to the stationary intensity distribution $\mathscr{P}(I)$. It can be measured by repeatedly counting the time it takes for the intensity, initially at some value below I_1, to exceed the value I_2 for the first time. We will refer to ρ as a switching-time distribution function.

A useful relation between ρ and P can be derived by differentiating (20) with respect to T, substituting the right-hand side of (17), performing one partial integration and, finally, the use of the fact that $\mathscr{P}(I)$ is the stationary solution of (1), i.e.,

$$\frac{1}{2}\frac{d}{dI}[\mathscr{D}(I)\mathscr{P}(I)]=\mathscr{B}(I)\mathscr{P}(I)\ . \tag{21}$$

We then arrive at

$$\frac{\partial}{\partial T}\rho(T;I_1,I_2)=\frac{\tfrac{1}{2}\mathscr{D}(I)\mathscr{P}(I)\frac{\partial}{\partial I}P(T;I,I_2)\Big|_0^{I_1}}{\int_0^{I_1}dI\,\mathscr{P}(I)} =\frac{\mathscr{D}(I_1)\mathscr{P}(I_1)\frac{\partial}{\partial I_1}P(T;I_1,I_2)}{2\int_0^{I_1}dI\,\mathscr{P}(I)}\ , \tag{22}$$

where the last equality follows from $\mathscr{D}(0)=0$. By integrating (22), while using the fact that $\rho(0;I_1,I_2)=0$ for $I_1\neq I_2$, we find

$$\rho(T;I_1,I_2)=\frac{\mathscr{D}(I_1)\mathscr{P}(I_1)}{2\int_0^{I_1}dI\,\mathscr{P}(I)}\frac{\partial}{\partial I_1}\int_0^T dT'P(T';I_1,I_2)\ , \tag{23}$$

which is the desired relation.

III. ANALYTIC EXPRESSIONS FOR THE FPT DISTRIBUTIONS

A. General results for the moments of P

In order to solve (17) for $P(T;I_1,I_2)$ it is convenient to consider the corresponding moment-generating function

$$M(z;I_1,I_2)=\int_0^\infty dT\,e^{zT}P(T;I_1,I_2)\ , \tag{24}$$

which satisfies the differential equation

$$\left[\tfrac{1}{2}\mathscr{D}(I_1)\frac{\partial^2}{\partial I_1^2}+\mathscr{B}(I_1)\frac{\partial}{\partial I_1}+z\right]M(z;I_1,I_2)=0\ . \tag{25}$$

In view of (18) and (19) we must solve (25) subject to the conditions

$$M(z;I_2,I_2)=1 \tag{26}$$

and

$$\mathscr{B}(0)\frac{\partial}{\partial I_1}M(z;I_1,I_2)\bigg|_{I_1=0}=-zM(z;0,I_2)\ . \tag{27}$$

Furthermore, since P is a probability distribution, the following equality should be satisfied for each I between I_1 and I_2:

$$P(T;I_1,I_2)=\int_0^\infty dT'P(T';I_1,I)P(T-T';I,I_2)\ , \tag{28}$$

expressing the fact that diffusion from I_1 to I_2 is the same as diffusion from I_1 to some intermediate intensity I, and from there on to I_2. In (28) it is understood that $P(T-T';I,I_2)=0$ if $T'>T$. A direct consequence of (28) is that M factorizes into

$$M(z;I_1,I_2)=M(z;I_1,I)M(z;I,I_2)\ , \tag{29}$$

for each I between I_1 and I_2, and this implies the existence of a function $G(z;I)$ such that

$$M(z;I_1,I_2)=\exp\left[\int_{I_1}^{I_2}dI\,G(z;I)\right]\ . \tag{30}$$

By substitution of (30) in (25), and using (21), one can obtain the differential equation

$$K(z;I)^2-\mathscr{D}(I)\mathscr{P}(I)\frac{\partial}{\partial I}K(z;I)+2\mathscr{D}(I)\mathscr{P}(I)^2z=0\ , \tag{31}$$

where $K(z;I)$ is related to $G(z;I)$ by

$$K(z;I)=\mathscr{D}(I)\mathscr{P}(I)G(z;I)\ . \tag{32}$$

In view of condition (27), Eq. (31) must be solved subject to

$$\lim_{I\to 0}[\mathscr{B}(I)K(z;I)-\mathscr{D}(I)\mathscr{P}(I)z]=0\ . \tag{33}$$

Furthermore, since $M(0;I_1,I_2)=1$, we also have

$$K(0;I)=0\ . \tag{34}$$

We will solve (31) by writing $K(z;I)$ as a power series in z,

$$K(z;I)=\sum_{n=1}^{\infty}K_n(I)z^n\ . \tag{35}$$

By subsitution of (35) in (31) we find

$$\frac{d}{dI}K_1(I)=2\mathscr{P}(I)\ , \tag{36}$$

$$\frac{d}{dI}K_n(I)=\frac{1}{\mathscr{D}(I)\mathscr{P}(I)}\sum_{\substack{p,q\\ p+q=n}}K_p(I)K_q(I)\quad (n=2,3,4,\ldots)\ . \tag{37}$$

The general solution to (36) is

$$K_1(I)=2\int_0^I dI'\mathscr{P}(I')+C_1\ ,$$

where C_1 is a constant. In view of condition (33), in which it should be realized that $\mathscr{D}(I)$ is proportional to I, the constant C_1 must vanish, or

$$K_1(I)=2\int_0^I dI'\mathscr{P}(I')\ . \tag{38}$$

The solution to (37) is

$$K_n(I)=\int_0^I dI'\frac{\sum_{\substack{p,q\\ p+q=n}}K_p(I')K_q(I')}{\mathscr{D}(I')\mathscr{P}(I')}\quad (n=2,3,4,\ldots) \tag{39}$$

where for reasons similar as for C_1, the constants again vanish. The problem of determining $M(z;I_1,I_2)$ is, in principle, solved now, apart from the actual calculation of the integrals. It follows directly from (30), (32), and (38) that the mean first-passage time from I_1 to I_2 is given by

$$\langle T\rangle_{I_1,I_2}=\left.\frac{\partial M(z;I_1,I_2)}{\partial z}\right|_{z=0}$$

$$=2\int_{I_1}^{I_2}\frac{dI}{\mathscr{D}(I)\mathscr{P}(I)}\int_0^I dI'\mathscr{P}(I')\ , \tag{40}$$

which is a well-known result.[1,5,7,8] Higher moments can be obtained with the use of the general rule

$$\langle T^n\rangle_{I_1,I_2}=\left.\frac{\partial^n M(z;I_1,I_2)}{\partial z^n}\right|_{z=0}\ . \tag{41}$$

By repeatedly using (39), the moments can be expressed in terms of multiple integrals, the number of which rapidly increases with increasing order n. General expressions for the moments can be found in Ref. 1, Eq. (7).

In Figs. 3 and 4 we give some numerical results for the mean FPT $\langle T\rangle_{0,I_2}$, obtained by numerical evaluation of

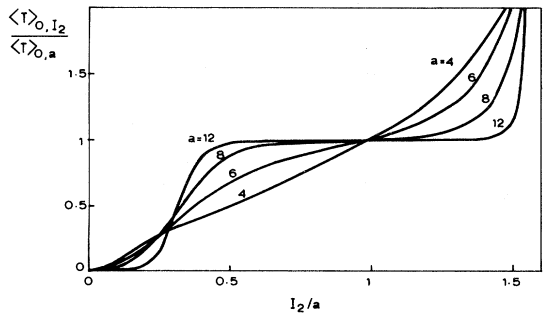

FIG. 3. Normalized mean FPT $\langle T\rangle_{0,I_2}/\langle T\rangle_{0,a}$ vs I_2/a for $a=4$, 6, 8, and 12. Absolute values of $\langle T\rangle_{0,a}$ are 1.77, 3.70, 15.2, and 3850, respectively. Coupling constant ξ equals 2 in all cases.

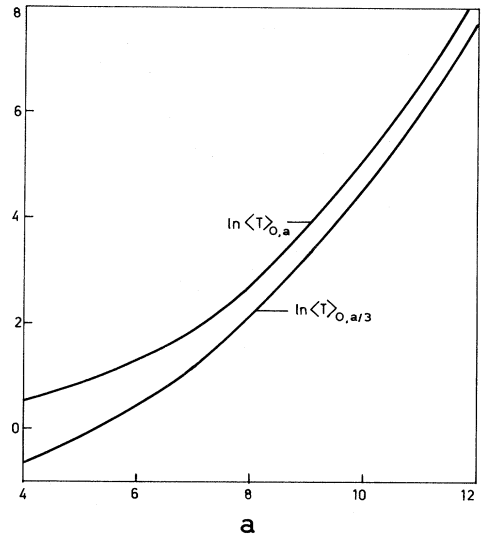

FIG. 4. $\ln\langle T\rangle_{0,I_2}$ vs pump parameter a for $I_2=a/3$ and a, and $\xi=2$.

the double integral in (40). The curves in Fig. 3 are all normalized to the mean FPT $\langle T\rangle_{0,a}$, while the respective values of the latter are mentioned in the figure caption. We recall that for $a=4$ the potential has one single minimum, namely, at $I=0$ (see Fig. 1); for $a\geq 8$ there are two well-resolved minima at $I=0$ and $I\simeq a$, respectively, separated by a maximum at $I\simeq a/3$, whereas the case $a=6$ is an intermediate case in which the potential does have two minima, one of which, however, is not well resolved yet. It can be seen from Fig. 3 that if the potential has two well-resolved minima, i.e., the cases $a=8$ and 12, the normalized FPT starts to increase slowly as I_2 increases, but then rises swiftly to 1 when $I_2/a\sim\frac{1}{3}$ and keeps this value in a relatively large interval around $I_2/a=1$, until for values of I_2/a well beyond 1 the mean FPT drastically rises. This behavior reflects the intuitive idea that once the mode intensity has dwelled from 0 to a value just across the maximum of the potential barrier, it is very likely to diffuse further to any value around $I/a=1$, that is, the intensity is likely to be captured in the potential well around $I=a$.

This can also be discussed by means of an approximate expression for $\langle T\rangle_{0,I_2}$ that can be derived when the laser is operating well above threshold, while the coupling constant ξ is not too close to 1, or more precisely, when $(\xi-1)a^2\gg 1$. We then find, at least for values of I_2 that are not too close to 0 nor much larger than a,

$$\frac{\langle T\rangle_{0,I_2}}{\langle T\rangle_{0,a}}\simeq\tfrac{1}{2}\mathrm{erfc}\left[\frac{(\xi^2-1)^{1/2}}{2}(I_B-I_2)\right]\ , \tag{42}$$

where

$$\langle T\rangle_{0,a}=\frac{\sqrt{\pi}(\xi+1)^{1/2}}{(\xi-1)^{3/2}a^2}\exp\left[\frac{1}{4}\frac{(\xi-1)}{(\xi+1)}a^2\right]\ , \tag{43}$$

and $I_B\simeq a/(1+\xi)$ was recognized in (13) as the intensity separating the on and off state. Taking $I_2=I_B$, we find that $\langle T\rangle_{0,I_B}$ assumes half the value given in the right-

hand side of (43), in exact agreement with a corresponding result obtained by Ref. 2 [see Eq. (29b) in this reference].

The presence of the erfc function in (42) explains the shape of the curves in Fig. 3 for large a: in a relatively narrow region given by $|I_B-I_2|/a \lesssim 2/(\xi^2-1)^{1/2}a$, the erfc function jumps from 0 to 2. So, for sufficiently large values of the parameter $(\xi^2-1)^{1/2}a$ we can recognize two well-defined levels for the mean FPT curves and we can unambiguously define the mean off-on switching time $\langle T\rangle_{\text{off}}$ as the value of $\langle T\rangle_{0,I_2}$ corresponding to the upper level. We therefore propose for the mean switching time $\langle T\rangle_{\text{off}}$ a value that is precisely twice as large as the value adopted in Ref. 2. The mean switching time is thus twice as large as the mean FPT for reaching the discriminating intensity I_B, which is an obvious consequence of the fact that once the intensity has reached the value I_B, the mode can either be turned on or off with equal probability. Only when the intensity has passed I_B by an amount of $2/(\xi^2-1)^{1/2}$, the mode can be said to be turned on with probability almost equal to unity.

B. Asymptotic expressions for P and ρ valid for large a

When the potential $V(I)$ has two well-resolved minima, that is, has a high barrier in between, the integrations in (39) can be performed after some approximations. If I_M is the intensity for which the barrier maximum is reached (see Fig. 5), then the approximate method is based on the observation that under the above-mentioned circumstances the function $1/\mathscr{P}(I)$ is sharply peaked at $I=I_M$ while the function $\int_0^I dI'\mathscr{P}(I')$ will depend only weakly on I when I varies around I_M. The details of the method are given in the Appendix and it will suffice here to give the results. We mention, in addition, that the error made in this approximation is, roughly speaking, proportional to the number of integrals involved. This means that expressions for the higher-order moments thus obtained become less accurate with increasing order. On the other hand, the accuracy will increase with increasing barrier height, that is, with increasing values of the parameter $(\xi-1)a^2$.

Following the method described in the Appendix we find, as long as I is not close to 0, the simple result

$$M(z;0,I)\simeq\frac{1}{1-z\langle T\rangle_{0,I}}\ , \tag{44}$$

where $\langle T\rangle_{0,I}$ is given by (40) with $I_1=0$ and $I_2=I$. From (44) it follows immediately that, in this approximation,

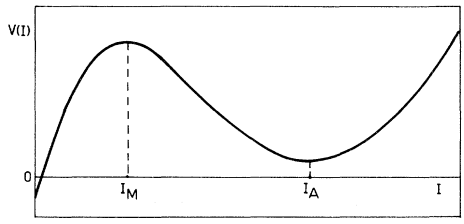

FIG. 5. Schematic illustration of the potential when the laser operates not too close to threshold ($a\gtrsim 6$). There are two minima at $I=0$ and I_A, which are separated by a barrier. Highest point of the barrier is reached for $I=I_M$. Approximate values for I_m and I_A are $a/(\xi+1)$ and a, respectively.

$$P(T;0,I)\simeq\frac{1}{\langle T\rangle_{0,I}}\exp\left[-\frac{T}{\langle T\rangle_{0,I}}\right]\ . \tag{45}$$

According to (29) we can write, for $I_1\le I_2$,

$$M(z;I_1,I_2)=\frac{M(z;0,I_2)}{M(z;0,I_1)}\ .$$

Hence, by substitution of (44), while assuming that both I_1 and I_2 are not too close to 0, we find

$$M(z;I_1,I_2)\simeq\frac{1-z\langle T\rangle_{0,I_1}}{1-z\langle T\rangle_{0,I_2}}\ , \tag{46}$$

or

$$P(T;I_1,I_2)\simeq\frac{\langle T\rangle_{0,I_1}}{\langle T\rangle_{0,I_2}}\delta(T)+\frac{\langle T\rangle_{I_1,I_2}}{\langle T\rangle_{0,I_2}^2}\exp\left[-\frac{T}{\langle T\rangle_{0,I_2}}\right]\ . \tag{47}$$

Let us now discuss the validity of these results.

First of all, we notice that the right-hand side of (45) does not vanish for $T=0$, but assumes its largest value there. Since it will take a finite time for the intensity to dwell from 0 to I_2, $P(T;0,I_2)$ should identically vanish for $T=0$. We conclude, therefore, that (45) makes no sense for small values of T. This is in agreement with the observation that the small-time behavior of $P(T;0,I_2)$ involves all moments of P, the accuracies of which, however, decrease with increasing order. A similar reasoning applies to (47) and, especially, the term proportional to $\delta(T)$ cannot be taken seriously. It will be shown later, when the short-time behavior is explicitly dealt with, that the delta function is merely a crude representation of a narrow-peaked function which reaches its maximum after a time that is much shorter than the mean FPT.

We will now derive an expression for $\rho(T;I_1,I_2)$. In view of (23) we can write for the moment-generating function $m(z;I_1,I_2)$ of ρ

$$m(z;I_1,I_2)=\frac{-\mathscr{D}(I_1)\mathscr{P}(I_1)}{2z\int_0^{I_1}dI\,\mathscr{P}(I)}\frac{\partial}{\partial I_1}M(z;I_1,I_2)\ , \tag{48}$$

which, after substitution of (46), performing the differentiation, and using (30) and (32), can be written as

$$m(z;I_1,I_2)\simeq\frac{K(z;I_1)}{2z\int_0^{I_1}dI\,\mathscr{P}(I)}\frac{M(z;0,I_2)}{M(z;0,I_1)}\ . \tag{49}$$

After substitution of (A8) and (A9) and using (40) we find

$$m(z;I_1,I_2)\simeq\frac{1}{1-\langle T\rangle_{0,I_2}z}\ , \tag{50}$$

where it is assumed that I_1 and I_2 are not close to 0, $I_1\le I_M$ and $I_1<I_2$. Hence we find for ρ in this approximation

$$\rho(T;I_1,I_2)\simeq\frac{1}{\langle T\rangle_{0,I_2}}\exp\left[-\frac{T}{\langle T\rangle_{0,I_2}}\right]\ , \tag{51}$$

valid for not too small values of T. It can be argued that (51), although derived under the assumption that I_1 is not

close to 0, is still valid for I_1 close to 0. We refer, therefore, to the definition (20) of ρ, which for small I_1 leads to

$$\rho(T;I_1,I_2)=\frac{\int_0^{I_1} dI\,\mathscr{P}(I)P(T;I,I_2)}{\int_0^{I_1} dI\,\mathscr{P}(I)}\simeq P(T;0,I_2)$$

$$\simeq\frac{1}{\langle T\rangle_{0,I_2}}\exp\left[-\frac{T}{\langle T\rangle_{0,I_2}}\right],$$

i.e., a result identical to (51). Therefore, we may safely conclude that (51) is a good approximation for all values of $I_1\leq I_M$ and $I_1<I_2$, as long as I_2 is not too close to 0 and for not too small values of T.

At first sight, it may seem surprising that $\rho(T;I_1,I_2)$ as given by (51) is independent of I_1. However, this is indeed to be expected when realizing that the approximations were made under the assumption of well-resolved potential wells. This means that $\mathscr{P}(I)$ is sharply peaked at $I=0$, so that the main contributions to ρ come from initial intensities close to 0. It will therefore appear as if by far the majority of first-passage events at I_2 are due to diffusion from $I=0$, at least after a short time. So, for not too small times T the distribution $\rho(T;I_1,I_2)$ will be insensitive for the actual discriminating level I_1 and, in fact, be equal to the FPT distribution $P(T;0,I_2)$. For small times, however, we must expect that ρ will be very sensitive to variations of I_1, as will be discussed in Sec. III C.

C. Asymptotic expressions for P and ρ valid for small T

Since $M(-s;I_1,I_2)$ is the Laplace transform of $P(T;I_1,I_2)$ with respect to T, it is useful, when studying the short-time behavior of P, to obtain an expression for $M(-s;I_1,I_2)$ that is valid for large positive values of s. With this in mind we now write, instead of (35), the function K alternatively as

$$K(-s;I)=\sqrt{s}\sum_{n=0}^{\infty}\frac{L_n(I)}{s^{n/2}}\ . \tag{52}$$

By substitution of (52) in (31) we find

$$L_0(I)=-\mathscr{P}(I)\sqrt{2\mathscr{D}(I)} \tag{53}$$

and

$$\sum_{\substack{p,q\\ p+q=n}} L_p(I)L_q(I)$$

$$=\mathscr{D}(I)\mathscr{P}(I)\frac{d}{dI}L_{n-1}(I)\quad(n=1,2,3,\ldots)\ . \tag{54}$$

The choice of the minus sign in (53) is required in order to guarantee the boundedness of M for $s\to\infty$.

By using (32) and by substitution of (52) in (30), while neglecting contributions to $K(-s,I)$ of order $1/\sqrt{s}$ and smaller, we obtain

$$M(-s;I_1,I_2)$$

$$=\left[\frac{L_0(I_2)}{L_0(I_1)}\right]^{1/2}\exp\left[-\sqrt{2s}\int_{I_1}^{I_2}\frac{dI}{\sqrt{\mathscr{D}(I)}}\right], \tag{55}$$

with L_0 given by (53). Putting $\mathscr{D}(I)=8I$ and substituting for L_0, (55) can be written as

$$M(-s;I_1,I_2)=\left[\frac{\mathscr{P}(I_2)}{\mathscr{P}(I_1)}\right]^{1/2}\left[\frac{I_2}{I_1}\right]^{1/4}$$

$$\times\exp[-\sqrt{s}\,(\sqrt{I_2}-\sqrt{I_1})]\ . \tag{56}$$

The inverse Laplace transform of (56) yields[10]

$$P(T;I_1,I_2)$$

$$=\frac{1}{2\sqrt{\pi}}\left[\frac{\mathscr{P}(I_2)}{\mathscr{P}(I_1)}\right]^{1/2}\left[\frac{I_2}{I_1}\right]^{1/4}\frac{(\sqrt{I_2}-\sqrt{I_1})}{T^{3/2}}$$

$$\times\exp\left[\frac{-(\sqrt{I_2}-\sqrt{I_1})^2}{4T}\right], \tag{57}$$

which is valid for $T\to 0$. The largest value of T for which (57) will be still a good approximation becomes smaller as I_1 decreases. Namely, it can be seen that all terms with $n\geq 1$ in the expansion (52) diverge as $(sI_1)^{-(n-1)/2}$ when I_1 approaches 0. Therefore, (56) is valid for $s\gg I_1^{-1}$ and hence (57) is valid for $T\ll I_1$.

In order to derive an asymptotic expression for $P(T;0;I_2)$ we will again use a different method. Namely, when I is close to 0, the potential $V(I)$ can be approximated by a linear function,

$$V(I)\simeq V(0)+BI\ , \tag{58}$$

where, according to (11), the constant B is given by

$$B=\tfrac{1}{2}a(\xi-1)+\frac{\xi}{\sqrt{\pi}}\frac{e^{-a^2/4}}{1+\mathrm{erf}(a/2)}\ . \tag{59}$$

This linear approximation for $V(I)$ corresponds to a linear approximation for the drift $\mathscr{B}(I)$. By using (10) we find

$$\mathscr{B}(I)=4-4BI\ . \tag{60}$$

The differential equation (25) for M can, therefore, be approximated by

$$\left[I_1\frac{\partial^2}{\partial I_1^2}+(1-BI_1)\frac{\partial}{\partial I_1}-\frac{s}{4}\right]M(-s;I_1,I_2)=0\ , \tag{61}$$

provided that I_1 is close to 0. Equation (61) is Kummer's equation[9] and is exactly solvable. Assuming now that I_2 is also close to 0, the solution to (61), satisfying (26) and (27), is given by

$$M(-s;I_1,I_2)=\frac{\Phi(s/4B,1,BI_1)}{\Phi(s/4B,1,BI_2)}\ , \tag{62}$$

where Φ is Kummer's function,[9] i.e.,

$$\Phi(a,b,x)$$

$$\equiv 1+\frac{ax}{b\,1!}+\frac{a(a+1)x^2}{b(b+1)2!}+\frac{a(a+1)(a+2)x^3}{b(b+1)(b+2)3!}+\cdots\ .$$

Using the appropriate asymptotic expression for Kummer's function,[9] we find that

$$M(-s;0,I_2)\to\sqrt{2\pi}e^{-(1/2)BI_2}(sI_2)^{1/4}e^{-\sqrt{sI_2}}\ , \tag{63}$$

for $s\gg 2B$ and provided that $BI_2\geq 1$. We will now argue that (63) is expected to be a good approximation even when I_2 lies outside the region where the potential can be approximated by (58). Therefore, we choose an intensity I

between 0 and I_2 such that I is large enough that $M(-s;I,I_2)$ is given by (56) and small enough that $M(-s;0,I)$ can be approximated by (63). Assuming that such a value of I can indeed be found, we can now use (29) and write

$$M(-s;O,I_2)=M(-s;0,I)M(-s;I,I_2)\ , \tag{}$$

where $M(-s;0,I)$ is given by (63) and $M(-s;I,I_2)$ by (56). The result can be written in the form

$$M(-s;0,I_2) \sim \sqrt{2\pi}\exp[\tfrac{1}{2}V(I)-\tfrac{1}{2}BI-\tfrac{1}{2}V(I_2)](sI_2)^{1/4} \times\exp(-\sqrt{sI_2})\ . \tag{64}$$

Since $V(I)$ has been approximated by (58), the I-dependent terms in the right-hand side of (64) cancel consistently and the result can be written as

$$M(-s;0,I_2) \sim \sqrt{2\pi}\left[\frac{\mathscr{P}(I_2)}{\mathscr{P}(0)}\right]^{1/2}(sI_2)^{1/4}\exp(-\sqrt{sI_2})\ . \tag{65}$$

Let us discuss the conditions under which this expression is valid. Since we have used (63) with $I_2=I$ and (56) with $I_1=I$, the conditions are $s\gg 2B$, $s\gg I^{-1}$ while $BI\geq 1$ and $I\leq I_2$. Since the condition $s\gg I^{-1}$ is already implied by $s\gg 2B$ and $BI\geq 1$, we conclude that (65) is valid for $s\gg 2B$ and $BI_2\geq 1$.

By taking the inverse Laplace transform of (65) we find[10]

$$P(T;0,I_2)\sim 2\left[\frac{\mathscr{P}(I_2)}{\mathscr{P}(0)}\right]^{1/2}\exp\left[\frac{-I_2}{8T}\right]W_{1;1/4}\left[\frac{I_2}{4T}\right]\ , \tag{66}$$

where $W_{1;1/4}$ is Whittaker's W function.[9] Using the asymptotic expansion of Whittaker's function for large arguments,[9] we readily obtain

$$P(T;0,I_2)\sim\frac{1}{2}\left[\frac{\mathscr{P}(I_2)}{\mathscr{P}(0)}\right]^{1/2}I_2\frac{e^{-I_2/4T}}{T^2}\ , \tag{67}$$

which is valid for $T\ll 1/2B$ and as long as $BI_2\geq 1$. Equations (57) and (67) are the desired asymptotic expressions for P. The important difference between the two expressions is that $P(T;0,I_2)$ has a T^{-2} proportionality whereas $P(T;I_1,I_2)$ is proportional to $T^{-3/2}$. Since they are both proportional also to, in fact, the same exponential factor, the former distribution rises relatively faster than the latter as T increases from 0. This difference in behavior is related to the fact that at $I_1=0$, there is no diffusion while the drift will always push the intensity initially in the direction of I_2. If, on the other hand, I_1 is well above 0, then there is always a chance that the intensity will initially decrease, that is, move away from I_2, so that it will take a relatively longer time to reach I_2.

Let us finally derive asymptotic expressions for $\rho(T;I_1,I_2)$. Substituting (57) in (23) and performing the integration over T, we find

$$\rho(T;I_1,I_2)=\frac{4I_1\mathscr{P}(I_1)}{\int_0^{I_1}dI\,\mathscr{P}(I)}\frac{\partial}{\partial I_1}\left[\left[\frac{\mathscr{P}(I_2)}{\mathscr{P}(I_1)}\right]^{1/2}\left[\frac{I_2}{I_1}\right]^{1/4}\operatorname{erfc}\left[\frac{\sqrt{I_2}-\sqrt{I_1}}{2\sqrt{T}}\right]\right]\ . \tag{68}$$

After performing the differentiation and using (21), the final answer can be written as

$$\rho(T;I_1,I_2)=\frac{2[\mathscr{P}(I_1)\mathscr{P}(I_2)]^{1/2}(I_1I_2)^{1/4}}{\int_0^{I_1}dI\,\mathscr{P}(I)}\left[\frac{\exp\left[-\frac{(\sqrt{I_2}-\sqrt{I_1})^2}{4T}\right]}{\sqrt{\pi T}}-\frac{\mathscr{B}(I_1)-2}{4\sqrt{I_1}}\operatorname{erfc}\left[\frac{\sqrt{I_2}-\sqrt{I_1}}{2\sqrt{T}}\right]\right]\ . \tag{69}$$

This expression is valid for $T\ll T_1$ and $I_2>I_1$. For $I_1=0$ we have, according to (20),

$$\rho(T;0,I_2)=P(T;0,I_2)\ , \tag{70}$$

where $P(T;0,I_2)$ is given by (67). According to (69), the dominant contribution to $\rho(T;I_1,I_2)$ is, apart from the exponential, proportional to $T^{-1/2}$, whereas for $\rho(T;0,I_2)$ this proportionality factor is T^{-2}. The difference between the two ρ distributions is therefore more pronounced than between the P distributions.

As an illustration of the various asymptotic results some plots are given. In Fig. 6 we have drawn the P and ρ function as given by the small-time asymptotic results (57) and (69), respectively, as well as the corresponding large-time exponentials. The parameter values are $a=6$, $\xi=2$, $I_1=1$, $I_2=2$, $\langle T\rangle_{0,1}=0.52$, and $\langle T\rangle_{0,2}=1.61$. The FPT distribution P is sharply peaked and assumes values much larger than the exponential. Such overshoot effects tend to become larger when I_1 and I_2 are closer to each other, in which case the peak tends to become higher and narrower. In fact, the δ function in (47) is a crude representation of this narrow peak. For the switching time ρ, the small-time peak behavior is mostly washed out.

In Fig. 7 we have drawn the FPT distribution $P(T;0,I_2)$ given by (67) and the corresponding exponential (45) with parameter values $a=6$, $\xi=2$, $I_2=0.5$, and $\langle T\rangle=0.18$. P is seen to approach the exponential closely without showing the narrow and high peak as in Fig. 6. A slight overshoot, however, is expected in view of normalization considerations. In Sec. IV we will confront the asymptotic results with various histograms obtained by numerical simulation of the FPT problem.

IV. NUMERICAL RESULTS

The algorithm used in the numerical simulation of the diffusion process described by the Langevin equation (2) is given by

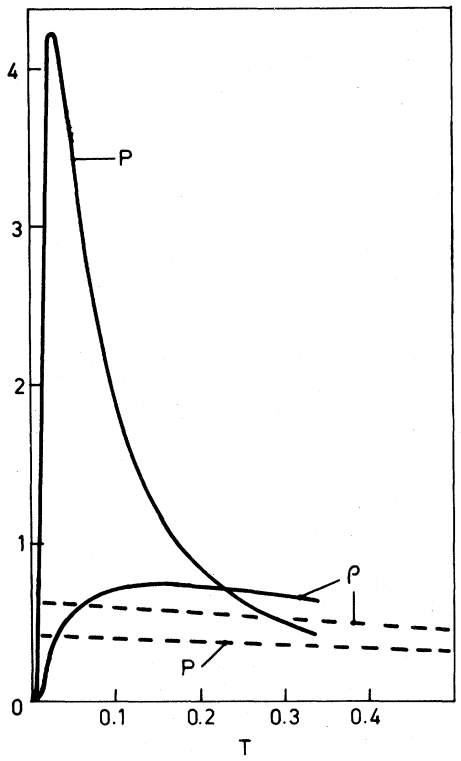

FIG. 6. P and ρ curves for $a=6$, $\xi=2$, $I_1=1$, and $I_2=2$. Solid P curve is the small-time asymptotic result (57); the dashed P curve is the corresponding large-time exponential, that is, the second term in the right-hand side of (47). Solid ρ curve is the small-time asymptotic result (69) and the dashed ρ curve is the corresponding exponential (45). Exponentials are based on the calculated values $\langle T\rangle_{0,1}=0.52$ and $\langle T\rangle_{0,2}=1.61$.

$$I(t+\tau)=[\mathscr{B}(I(t))+8Y]\tau\,, \tag{71}$$

where Y is distributed according to the one-parameter gamma distribution

$$\varphi(Y)=Y^{I/8\tau-1}e^{-Y}/\Gamma(I/8\tau) \tag{72}$$

and τ is the time interval step. Starting at $t=0$ with intensity I_1, the algorithm (71) is subsequently used until after n steps the intensity becomes larger than I_2 $(I_2>I_1)$ for the first time, or until the total number of steps exceeds a given value N. In the first case we conclude that a first-passage event at I_2 took place at a time T between $(n-1)\tau$ and $n\tau$. In the second case we can only say that $T>N\tau$. Thus, a histogram can be obtained by repeating the above-described procedure M times, where M is a large number. It should be emphasized however, that the limiting form of this histogram when $M\to\infty$ may systematically differ from the actual first-passage histogram. This follows from the observation that after each step only those events are counted for which the intensity exceeds I_2. However, there will be more of them, since all first-passage events that were directly followed by diffusion backwards to a value below I_2 are erratically discarded in this way. For instance, it can be shown that if $\varphi(Y)$ is a Gaussian distribution—which is, actually, the asymptotic form of φ when the shape parameter $I/8\tau\gg1$—precisely half of the actual first-passage events are counted.

This problem can, in principle, be overcome by multiplying the number of numerically obtained first-passage events by a certain factor, but an extra complication is that this factor will depend on the step number in a complicated way. Namely, in those cases in which an "undetected" first-passage event took place, the numerical integration is continued, whereas it should have been terminated. It can be seen that the calculation of the correction factor in the nth step involves n repeated incomplete gamma-function integrals and, therefore, becomes very complicated, if not impossible. We were able to avoid this calculation by following a more pragmatic way of interpreting the results, in which the numerically obtained first-passage histogram is not compared with the corresponding analytic expression $P(T;I_1,I_2)$ but rather with $P(T;I_1,I_2+\Delta)$, where Δ is a positive intensity shift, the value of which will depend on the actual value of the time interval step τ.

In order to discuss the effect of such a Δ, it should be realized that in the ideal case of an infinitesimally small τ in (71), the probability that $I\geq I_2$ will be vanishingly small. In the calculations, however, τ is always given a finite value and this means that after each integration step there remains a finite probability density $\mathscr{P}(I)$ for $I>I_2$. This probability density will be a decreasing function of I, but it will be vanishingly small only when $I-I_2$ is larger than, say, one diffusion length, or, $I-I_2>\sqrt{\mathscr{D}(I_2)\tau}$. It will, therefore, appear as if the numerically obtained results correspond to the FPT distribution at $I_2+\Delta$, where Δ will be of the order of $\sqrt{\mathscr{D}(I_2)\tau}$.

These ideas were fully confirmed by the numerical results. In all cases good agreement between the analytic and numerical results could be achieved in this way, where the optimum value of Δ was usually between 0.25 and 0.75 diffusion lengths.

It is instructive to realize that, since $\Delta\propto\sqrt{\tau}$ and since the FPT distributions $P(T;I_1,I_2)$ are very sensitive to small variations of I_2, the convergence of the calculated first-passage distributions when τ is taken smaller and

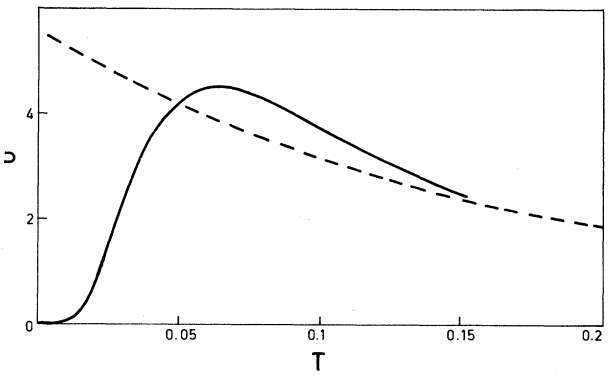

FIG. 7. P curves for $a=6$, $\xi=2$, $I_1=0$, and $I_2=0.5$. Solid curve is the small-time asymptotic result (67) and the dashed curve is the corresponding large-time exponential (45) with $\langle T\rangle_{0,0.5}=0.18$.

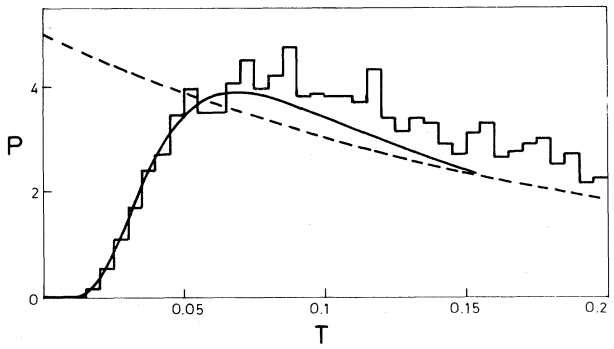

FIG. 8. FPT histogram and corresponding asymptotic functions for $a=6$, $\xi=2$, $I_1=0$, $I_2=0.55$, and the time interval step $\tau=0.005$. Total area of the histogram is 0.58 and the total number of first-passage events contributing to the histogram is 5803. Continuous solid curve is $P(T;0,0.55)$ as given by (67) and the dashed curve is the exponential (45) with $\langle T\rangle_{0,0.55}=0.20$.

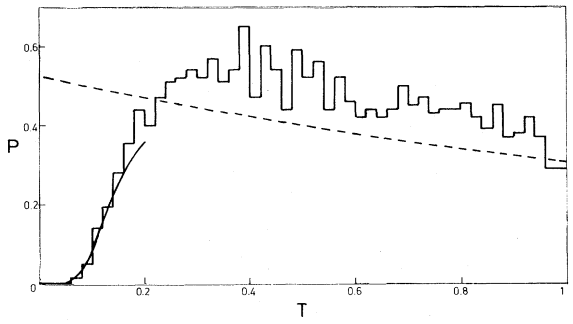

FIG. 10. FPT histogram and corresponding asymptotic functions for a=6, $\xi=2$, $I_1=0$, $I_2=2.2$, and $\tau=0.01$. Total area of the histogram is 0.40 and the total number of contributing events is 2595. Continuous solid curve is $P(T;0,2.2)$ as given by (67) and the dashed curve is the exponential (45) with $\langle T\rangle_{0,2.2}=1.91$.

smaller is very slow, which, in practice, leads to a conflicting confrontation between desired accuracy and computing time. Keeping the total number of first-passage events contributing to one histogram constant, the difference between the actual and the calculated distribution decreases by a factor f at the cost of a factor f^2 in computing time.

The numerically obtained histograms together with the asymptotic results for the corresponding FPT distributions are depicted in Figs. 8—13. All figures refer to the case $a=6$ and $\xi=2$ but differ in the combinations I_1 and I_2. The continuous solid curves represent the small-time asymptotic results and the dashed curves are the large-time exponential results for the FPT distributions. In Fig. 8 we have $I_1=0$ and $I_2=0.55$. The solid curve is $P(T;0,0.55)$ as given by (67). The exponential (dashed curve) is given by (45) in which for $\langle T\rangle$ the corresponding calculated value was taken as indicated in the figure caption. The agreement between the histogram and P is good for values of T up to 0.06, but from there on they differ systematically. This is indeed to be expected, since (67) is a good approximation only as long as $T\ll 1/2B \simeq 1/(\xi-1)a=0.167$.

A similiar behavior can be seen in Fig. 9 where $I_1=0$ and $I_2=1.2$. The exponential is seen to agree well with the histogram for $T\gtrsim 1$. There is also good agreement with the P curve, even for values of T up to $1/2B\simeq 0.167$. FPT results for $I_1=0$ and $I_2=2.2$ are shown in Fig. 10. In summary we have found that the FPT distributions from $I_1=0$ to I_2 show a steep increase proportional to $T^{-2}\exp(-I_2/4T)$ in the limit of small T, an exponential tail for large T, and a slight overshoot of the exponential for intermediate values of T.

Let us now turn to FPT results for cases with $I_1\neq 0$, which are shown in Figs. 11—13. The shape of the histograms and the positions of the maxima are well represented by the small-time asymptotic formula (57). Note, by comparing the differences in the horizontal and vertical scales of the three figures, the enormous narrowing and increase of height of the peaks as I_1 and I_2 approach each other. The height of each maximum can best be compared

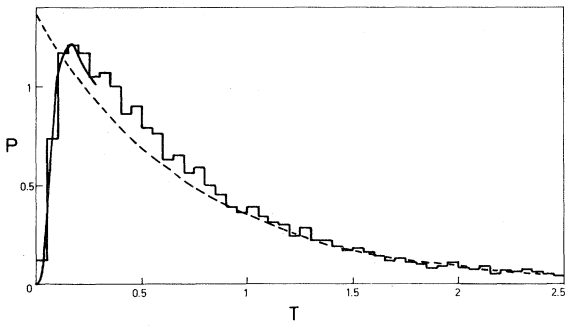

FIG. 9. FPT histogram and corresponding asymptotic functions for $a=6$, $\xi=2$, $I_1=0$, $I_2=1.2$, and $\tau=0.025$. Total area of the histogram is 0.97 and the total number of contributing events is 9741. Continuous solid curve is $P(T;0,1.2)$ as given by (67) and the dashed curve is the exponential (45) with $\langle T\rangle_{0,1.2}=0.73$.

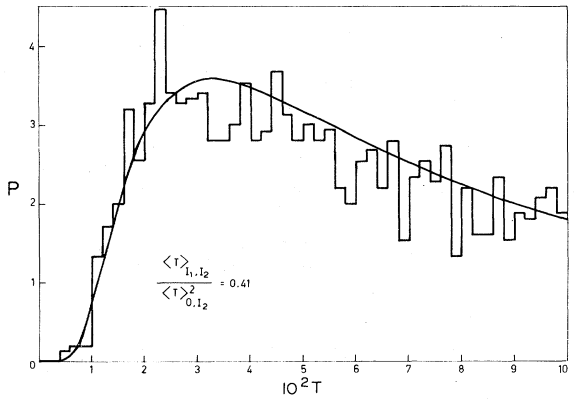

FIG. 11. FPT histogram and corresponding asymptotic function for $a=6$, $\xi=2$, $I_1=1$, $I_2=2.07$, and $\tau=0.001$. Total area of the histogram is 0.23 and the total number of contributing events is 1727. Continuous curve is $P(T;1,2.07)$ as given by (57).

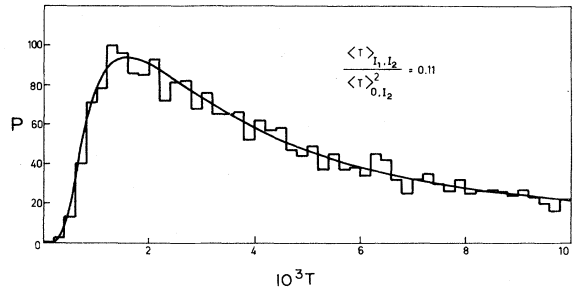

FIG. 12. FPT histogram and corresponding asymptotic function for $a=6$, $\xi=2$, $I_1=1.75$, $I_2=2.018$, and $\tau=10^{-4}$. Total area of the histogram is 0.47 and the total number of contributing events is 4700. Continuous curve is $P(T;1.75,2.018)$ as given by (57).

with the quantity $\langle T\rangle_{I_1,I_2}/\langle T\rangle^2_{0,I_2}$, which is the value of the corresponding exponential, i.e., the second term in the right-hand side of (47), for $T\to 0$. These values are indicated in the figures.

ACKNOWLEDGMENT

One of the authors (D.L.) would like to thank the Netherlands Organization for the Advancement of Pure Research [Nederlandse Organisatie voor Zuiver-Wetenschappelijk Onderzoek (Z.W.O.)] for financial support.

APPENDIX

The approximate method for performing the integrations in the right-hand side of (39) is based on the observation that if the potential minima are separated by a high barrier, the function $[\mathscr{P}(I)]^{-1}$ will show a steep increase from $I=0$ to $I=I_M$, a sharp maximum at I_M and a steep decrease from $I=I_M$ to $I\simeq a$. According to (39) with $n=2$ we have

$$K_2(I)=\int_0^I \frac{dI'K_1(I')^2}{\mathscr{D}(I')\mathscr{P}(I')} . \tag{A1}$$

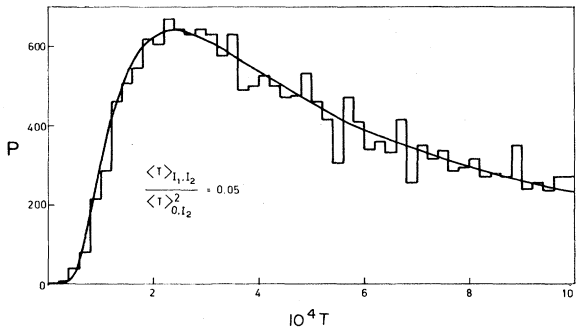

FIG. 13. FPT histogram and corresponding asymptotic function for $a=6$, $\xi=2$, $I_1=1.9$, $I_2=2.005$, and $\tau=10^{-5}$. Total area of the histogram is 0.39 and the total number of contributing events is 3898. Continuous curve is $P(T;1.9,2.005)$ as given by (57).

If $I\le I_M$ and I is not too close to 0 then $[\mathscr{P}(I')]^{-1}$ assumes its maximum at $I'=I$, while $K_1(I')$ and $\mathscr{D}(I')$ show only weak variations for $I'\lesssim I$. We can therefore write, to a first approximation,

$$K_2(I)\simeq\frac{K_1(I)^2}{\mathscr{D}(I)}\int_0^I\frac{dI'}{\mathscr{P}(I')} , \tag{A2}$$

and, by using the same arguments,

$$\begin{aligned}K_3(I)&=2\int_0^I\frac{dI'K_1(I')K_2(I')}{\mathscr{D}(I')\mathscr{P}(I')}\\&=2\int_0^I\frac{dI'K_1(I')}{\mathscr{D}(I')\mathscr{P}(I')}\int_0^{I'}\frac{dI''K_1(I'')^2}{\mathscr{D}(I'')\mathscr{P}(I'')}\\&\simeq\frac{2K_1(I)^3}{\mathscr{D}(I)^2}\int_0^I\frac{dI'}{\mathscr{P}(I')}\int_0^{I'}\frac{dI''}{\mathscr{P}(I'')}\\&=\frac{K_1(I)^3}{\mathscr{D}(I)^2}\left[\int_0^I\frac{dI'}{\mathscr{P}(I')}\right]^2 .\end{aligned} \tag{A3}$$

Generally, we find in this way

$$K_n(I)\simeq\frac{K_1(I)^n}{\mathscr{D}(I)^n}\left[\int_0^I\frac{dI'}{\mathscr{P}(I')}\right]^n$$
$$(n=1,2,\ldots \text{ and } 0\ll I\le I_M) . \tag{A4}$$

In the case $I_M\le I\lesssim a$ we can apply a similar approximation. The integrand in (A1) is now sharply peaked at $I'=I_M$, so that, to a first approximation,

$$K_2(I)\simeq\frac{K_1(I_M)^2}{\mathscr{D}(I_M)}\int_0^I\frac{dI'}{\mathscr{P}(I')} , \tag{A5}$$

or, generally,

$$K_n(I)\simeq\frac{K_1(I_M)^n}{\mathscr{D}(I_M)^{n-1}}\left[\int_0^I\frac{dI'}{\mathscr{P}(I')}\right]^{n-1}$$
$$(n=1,2,\ldots \text{ and } I_M\le I\lesssim a) . \tag{A6}$$

We can now substitute these expressions in the right-hand side of (35) and carry out the summation. This leads to

$$K(z;I)\simeq\begin{cases}\dfrac{K_1(I)z}{1-\dfrac{2zK_1(I)}{\mathscr{D}(I)}\displaystyle\int_0^I\frac{dI'}{\mathscr{P}(I')}}, & 0\ll I\le I_M\\[2ex]\dfrac{K_1(I_M)z}{1-\dfrac{2zK_1(I_M)}{\mathscr{D}(I_M)}\displaystyle\int_0^I\frac{dI'}{\mathscr{P}(I')}}, & I_M\le I\lesssim a .\end{cases} \tag{A7}$$

Consistent with the former approximations, we can write (A7) also as

$$K(z;I)\simeq\begin{cases}\dfrac{K_1(I)z}{1-\int_0^I \dfrac{dI'2zK_1(I')}{\mathscr{D}(I')\mathscr{P}(I')}}, & 0\ll I\leq I_M\\ \dfrac{K_1(I_M)z}{1-\int_0^I \dfrac{dI'2zK_1(I')}{\mathscr{D}(I')\mathscr{P}(I')}}, & I_M\leq I\lesssim a\ .\end{cases}\tag{A8}$$

Substitution of (A8) in (30), with the use of (32), yields, for $0\ll I\leq I_M$,

$$M(z;0,I)\simeq\exp\left[\int_0^I \frac{dI'2zK_1(I')}{\mathscr{D}(I')\mathscr{P}(I')}\frac{1}{1-\int_0^{I'}\frac{dI''2zK_1(I'')}{\mathscr{D}(I'')\mathscr{P}(I'')}}\right]$$
$$=\frac{1}{1-\int_0^I \frac{dI'2zK_1(I')}{\mathscr{D}(I')\mathscr{P}(I')}}=\frac{1}{1-z\langle T\rangle_{0,I}}\ .\tag{A9}$$

Similarly, for $I_M\leq I\lesssim a$, we can write

$$M(z;0,I)\simeq\exp\left[\int_0^I \frac{dI'2zK_1(I_M)}{\mathscr{D}(I')\mathscr{P}(I')}\frac{1}{1-\int_0^{I'}\frac{dI''2zK_1(I'')}{\mathscr{D}(I'')\mathscr{P}(I'')}}\right]$$
$$\simeq\exp\left[\int_0^I \frac{dI'2zK_1(I')}{\mathscr{D}(I')\mathscr{P}(I')}\frac{1}{1-\int_0^{I'}\frac{dI''2zK(I'')}{\mathscr{D}(I'')\mathscr{P}(I'')}}\right]$$
$$=\frac{1}{1-z\langle T\rangle_{0,I}}\ .\tag{A10}$$

Let us now qualitatively discuss the accuracy of these results. First of all, we had to exclude values of I close to 0. The precise lower bound on I follows from the requirement that $[\mathscr{P}(I)]^{-1}$ should be, roughly speaking, an order of magnitude larger than $[\mathscr{P}(0)]^{-1}$. Hence, the lowest value of I for which the approximation still makes sense will decrease when the pump parameter increases. Secondly, the number of approximations used to evaluate $K_n(I)$ increases with n and so will the error. Therefore, (A9) and (A10) will become less accurate with increasing z.

*Present address: Department of Electrical Engineering, Delft University of Technology, 2600-GA Delft, The Netherlands.

[1]R. Roy, R. Short, J. Durnin, and L. Mandel, Phys. Rev. Lett. 45, 1486 (1980).

[2]L. Mandel, R. Roy, and S. Singh, in *Optical Bistability,* edited by C. M. Bowden, M. Ciftan, and Th.R. Robl (Plenum, New York, 1981).

[3]P. Lett, W. Christian, S. Singh, and L. Mandel, Phys. Rev. Lett. 47, 1892 (1981).

[4]F. Haake, J. W. Haus, and R. Glauber, Phys. Rev. A 23, 3255 (1981).

[5]R. Bonifacio, L. Lugiato, J. D. Farina, and L. M. Narducci, IEEE J. Quantum Electron. QE-17, 357 (1981).

[6]S. Singh and L. Mandel, Phys. Rev. A 20, 2459 (1979).

[7]G. H. Weiss, in *Stochastic Processes in Chemical Physics,* edited by I. Oppenheim, K. E. Schuler, and G. H. Weiss (MIT, Cambridge, Mass., 1977), p. 361.

[8]G. S. Agarwal and S. R. Shenay, Phys. Rev. A 23, 2719 (1981).

[9]L. J. Slater, in *Handbook of Mathematical Functions,* edited by M. Abramowitz and I. Stegun (Dover, New York, 1970), Chap. 13.

[10]G. E. Roberts and H. Kaufman, *Table of Laplace Transforms* (Saunders, Philadelphia, 1966).